

## Experimental investigation of bi-stability in a vertically excited rectangular tank with finite liquid depth

N. Kaloumenos, A. Grammatikopoulos, C.C. Spandonidis & K.J. Spyrou

*School of Naval Architecture and Marine Engineering, National Technical University of Athens, Greece*

**ABSTRACT:** An experimental investigation on the generation and character of sloshing of a parametrically excited liquid inside a rectangular tank is reported. The focus is set on the phenomenon of liquid surface bi-stability, i.e. when, for identical excitation parameters' values, sloshing may or may not be activated, depending on the initial state of the surface when the excitation is applied. From an earlier theoretical investigation it had been conjectured that, on the plane of frequency versus amplitude of excitation, the area of bi-stability is located adjacently to the principal resonance region of the corresponding Mathieu-type system. This was produced from a nonlinear mathematical model focused on the first free surface mode, derived by eliminating higher modes through an adaptive mode-ordering scheme. The comparison against experimental results presented in the current paper corroborates that the theoretical predictions are fair. The experiments provide also evidence about the activation of higher modes and the occurrence of phenomena of mode competition.

### 1 INTRODUCTION

As “parametric sloshing” is meant the motion of a liquid’s free surface, triggered by an excitation that acts perpendicularly to the undisturbed free surface. As pointed out many years ago, for vibrating structures containing liquids such a phenomenon may sometimes incur catastrophic consequences (Dodge 1966). Ship motions along the gravity vector, thus parametrically exciting the transported liquids, arise physically in combination with other rectilinear or angular ship motions. Nevertheless, it is very useful to understand fundamentally the various ways in which sloshing motion can appear, especially when this happens quite unexpectedly.

The seminal investigation of Benjamin & Ursell (1954) produced a first glimpse of the stability chart associated with the behaviour of the free surface of a parametrically excited liquid. It was derived from a linear Mathieu-type equation. Whilst this captures the region of linear instability, it does not suffice for predicting the ensuing free surface elevations, yielding unrealistic infinite wave amplitudes inside the instability region. In a series of papers, Miles investigated parametric sloshing on the basis of an averaged Lagrangian approach, using weakly nonlinear models (see for example Miles 1994). Extending Miles’ approach, Decend (1995) and Decend & Craig (1995) found hysteresis due to competition between the “finite-amplitude” and the “flat-surface” solutions. Perinet et al. (2009) carried out three-dimensional simulations

for the full nonlinear viscous problem, up to relatively high excitation amplitude. They reproduced the remarkable square and hexagonal free surface patterns that had been experimentally captured earlier by Kityk et al. (2005). Also, the issue of mode competition had been investigated experimentally by Simonelli & Gollub (1989) and by Craik & Armitage (1995) for shallow depth tanks. A comprehensive collection of earlier efforts concerning the nonlinear behaviour of liquids carried in tanks of various shapes and subjected to parametric excitation can be found in Ibrahim (2005).

Research on the problem of liquid sloshing in a rectangular vertically excited tank was initiated recently in our group. A description of our modelling approach, implemented so far for 2-D cases, is presented in Spandonidis & Spyrou (2011 & 2012). It is based on the adaptive multimodal analysis introduced by Faltinsen & Timokha (2001, 2009), applied earlier for directly excited sloshing. Coupling of the model with a “continuation algorithm” of nonlinear dynamical systems corroborated that a bi-stability region exists, located entirely inside the domain where, from a linear perspective, the surface should appear as quiescent. This analysis revealed further that, in line with well-known behaviour of nonlinear parametrically excited systems, the lower boundary of the bi-stability region is defined by the locus of the folding points of the curve of limit-cycle amplitude. The intriguing feature of this region, yet a common one for those familiar with strongly nonlinear behaviour,

is that it is initial-conditions-dependent; i.e. one may obtain a stable wavy surface or a flat surface depending on how much disturbed the free surface had been when the harmonic excitation was firstly applied.

In the presented work the main objective was the experimental reproduction of parametric sloshing. The experiments were conducted using a shaking table facility discussed in a later section. Attention has been paid on activating wave modes only along the longer tank side. Even though complex excitation scenarios could easily be examined, at this stage was assumed harmonic vertical forcing with small to moderate amplitude. Excitation frequencies were kept around the frequency of principal resonance of the lowest mode (in reference to the longer side). Results have been compared against the relevant generic linear stability chart as well as against predictions obtained by the modal analysis method (that is briefly outlined in the following section). The applied mode ordering scheme leads to a fundamental core model comprised of a single, Mathieu type, 2nd order ordinary differential equation, presenting two third-order nonlinearities: one due to a product of elevation with the square of elevation velocity; and another due to a product of elevation squared with acceleration.

## 2 SUMMARY OF THEORETICAL RESULT

The height-to-length ratio of the considered rectangular tank is  $h/l = 0.4$ . The hydrodynamic problem has been formulated in terms of Laplace's equation for the velocity potential  $\Phi(y, z, t)$  applied throughout the fluid volume  $Q(t)$ . The well-known boundary conditions are enforced on the free surface  $\Sigma(t)$  and on the tank surface  $S(t)$ .

Faltinsen & Timokha (2001 & 2002) converted the governing equations into an infinite-dimensional system of ODEs, postulating Fourier series representations for describing surface's elevation  $\zeta(y, t)$  and the velocity potential  $\Phi(y, z, t)$ , as indicated below:

$$\zeta(y, t) = \sum_{i=1}^{\infty} \beta_i(t) f_i(y) \quad (1)$$

$$\Phi(y, z, t) = \sum_{i=1}^{\infty} R_i(t) \varphi_i(y, z) \quad (2)$$

$$\varphi_i(y, z) = \cos\left(\frac{\pi i}{l}\left(y + \frac{1}{2}l\right)\right) \times \frac{\cosh\left(\frac{\pi i(z)}{l}\right)}{\cosh\left(\frac{\pi i h}{l}\right)} \quad (3)$$

$$f_i(y) = \cos\left[\frac{\pi i\left(y + \frac{1}{2}l\right)}{l}\right], \quad i \geq 1 \quad (4)$$

The axes origin is fixed at the middle of the undisturbed surface. The  $y$  axis points to the right along the length of the tank and the  $z$  axis is vertical, pointing upwards.  $\beta_i(t)$  corresponds to the time-dependant free surface elevation that occurs due to the  $i$ th natural mode.

Keeping nonlinear terms up to third-order, applying a mode ordering scheme based on  $\beta_1 = \mathcal{O}(\varepsilon^{1/3})$ ,  $\beta_\mu = \mathcal{O}(\varepsilon)$ ,  $\mu > 1$  finally retaining  $\beta_1$  only, incorporating damping and assuming perpendicular harmonic excitation  $n_3 = n_{3a} \cos(\sigma t)$ , the infinite system of ODEs is reduced for purely vertical excitation to the following simple equation:

$$\ddot{\beta}_1 + 2\zeta_1 \sigma_1 \dot{\beta}_1 + \sigma_1^2 \left(1 - \frac{n_{3a} \sigma^2}{g} \cdot \cos(\sigma \cdot t)\right) \beta_1 + d_2 (\dot{\beta}_1 \beta_1^2 + \beta_1^2 \dot{\beta}_1) = 0 \quad (5)$$

where:

$$d_2 = \frac{\pi^2}{4} \left[1 - 2 \cdot \tan h\left(\frac{\pi h}{l}\right) \cdot \tan h\left(2\pi \frac{h}{l}\right)\right] \quad (6)$$

$\beta_1$  stands in this case for the time-dependant free surface elevation at  $y = -l/2$ ; i.e. at the left tank wall.  $\sigma_\mu$  is  $\mu$ th natural frequency and  $\delta$  is Kronecker's symbol; while  $d, t$  are functions of liquid's height-to-tank-length-ratio. It is apparent that omission of the nonlinear terms leads to a Mathieu-type system.

The mathematical model was coupled to the computational algorithm MATCONT (Doodge et al. 2003). This algorithm is much more than an ODE solver, allowing to trace efficiently steady-state solutions of Eq. 2 as one varies either the frequency ratio or the excitation amplitude (or even both simultaneously). Stability analysis yielded that the forcing-versus-frequency parameters' plane is divided into three areas. Area A is host to quiescent steady solutions: i.e. every vertical external excitation leads invariably, no matter what the initial state of the free surface was, to a flat liquid surface. Area B is the classical area of instability where the excitation generates free surface oscillation. Typical parametric oscillations associated with this area have frequency about half the forcing frequency. However, other much more complex responses can be found here too. Area C is the one where bi-stable behaviour is exhibited. The same external excitation leads either to a quiescent surface or to a wavy one, depending on the initial condition (determined through the initial values of  $\beta_1$  and  $\varphi$ ).

### 3 EXPERIMENTAL SETUP

In Figure 1 is shown the vibration testing facility (“shaking table”) of NTUA’s School of Naval Architecture and Marine Engineering. It is based on a table platform that is able to perform Six Degree Of Freedom (6-DOF) low frequency motions according to appropriate input time histories, emulating motions performed by ships in waves. The motions can reach amplitudes of 30° and 0.5 m. In Table 1 are collected the key features of the shaking table.

A *Labview* interface program reads or generates desired time histories and computes the appropriate actuator motions. To translate the platform’s calibration/measurement to real motion, real time PID loops are used that control the six actuators. Moreover a table-mounted Miniature Attitude Heading Reference System (AHRS) with GPS (Microstrain 3DM-GX3-35) reports to the main PC the exact position of the table at any time.



Figure 1. The shaking-table of the School of Naval Architecture and Marine Engineering, National Technical University of Athens.

Table 1. Shaking-table properties.

Table size	120 cm × 120 cm
Degrees of freedom	Six (6)
Max. payload	2 tons
Max. displacement in heave*	30 cm
Max. velocity in heave*	50 cm/s
Max. displ. in sway/surge*	30 cm
Max. velocity in sway/surge*	30 cm/s
Max. displ. in roll/pitch/yaw*	30 deg
Max. velocity in roll/pitch/yaw*	15 deg/s
Frequency range	0–8 Hz
Max acceleration, any axis	0.3 g

\*Reduced range when complex movements are performed.

Flow visualization is possible by the use of a high speed video system. This system consists of two high speed video cameras (Trouble-Shooter HR-color) with a resolution of 1280 × 1024 pixels and a maximum speed of 16,000 images per second that cooperate in a master/slave mode. A specialized software program (MIDAS 4.0) is used for event-capture camera control, synchronization with data sources, and automated monitoring.

The use of two PCD-300B sensor interfaces working in a master/slave mode enables the main PC to perform up to 16 different stress and force, pressure, acceleration and displacement measurements through the use of strain gages and transducers, respectively. DCS 100 A dynamic data acquisition software enables easy, interactive setting of measuring conditions and sensor information as well as monitoring of measuring data on numeric and various graph windows.

The tank that was used is shown in Figure 2. It was initially designed for cargo shift investigations (IMO 2012). The tank is made from non-coloured Perspex of 20 mm thickness to permit direct observation. Its size is 0.6 m × 0.4 m × 0.4 m (width × length × height). To keep the scenario close to the one that had been investigated by the theoretical approach (that is, to have finite liquid depth with  $h/l = 0.4$ ), we partly filled the tank with water up to 0.24 m height.

The geometry of the tank and the height of the liquid yield the natural frequencies of the system, which depend either on tank’s length or tank’s width (as a matter of fact in height-to-length and height-to-width ratio). In Tables 2 and 3 are presented the natural frequencies corresponding to the first few modes, for longitudinal and transverse waves. In general, complex wave formation can be observed, featuring combined longitudinal and transverse oscillations (one example is shown in Fig. 3).

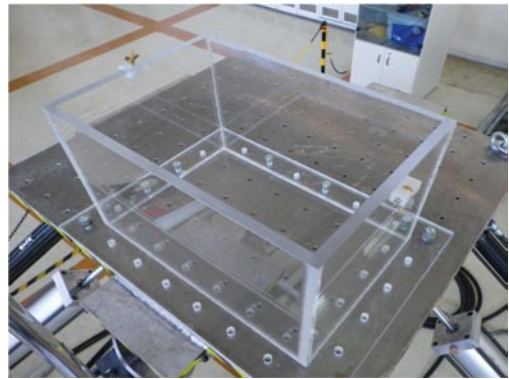


Figure 2. The orthogonal tank used for the experiments. It is made of Perspex of 20 mm thickness.

Table 2. Natural frequencies according to length of tank.

Odd modes	Value (rad/s)	Even modes	Value (rad/s)
1st	6.60811	2nd	10.0693
3rd	12.4069	4th	14.3333
5th	16.0257	6th	17.5553
7th	18.9619	8th	20.2712

Table 3. Natural frequencies according to width of tank.

Odd mode	Value (rad/s)	Even mode	Value (rad/s)
1st	8.5775	2nd	12.4069
3rd	15.2032	4th	17.5553
5th	19.6275	6th	21.5008
7th	23.2235	8th	24.82



Figure 3. Combined wave in longitudinal and in transverse direction. The tank is excited along the gravity vector. The tank presents a slight tilt around the transverse axis.

However, by restricting the range of excitation frequency around 13 rad/s (the frequency whereabout the vertex of the principal resonance region for the corresponding 2D tank should be expected) and keeping the excitation amplitude relatively low, the active modes associated with tank length can be relatively safely investigated, thus practically reducing the 3D to a 2D problem (nevertheless, some interference should still be expected since the 1st, 2nd and 3rd natural frequency of the transverse waves (see Table 3), are close to the borders of the investigated frequency range).

#### 4 EXPERIMENTAL RESULTS

Over 1200 “runs” were performed, separated into two sets, according to the initial free surface

condition. The excitation was always harmonic and along the vertical axis. A dense grid of excitation amplitudes and frequencies was examined. The frequency range was from 10 to 15 rad/s and the amplitude range was from 0 to 0.025 m. In order to verify the results, each experiment was repeated twice.

##### 4.1 Zero initial conditions

Sufficient time was allowed between consecutive runs in order for the free surface to calm down and thus achieve practically a “zero” initial condition for the ensuing run. The free surface dynamic response was labelled as “stable” if at the end of the “run” it appeared to be calm, like at the beginning of the run. It was “unstable” if, towards the end of the run, a non-decaying wavy surface was prevalent. In Figure 4 are shown time instances of liquid’s surface motion for two different excitations, exhibiting two different wave patterns: that are either the first (up) or the second (down) anti-symmetric modes (modes that correspond to the 3rd and 1st natural frequency or else to 3rd mode’s fundamental and 1st mode’s principal resonance, respectively).

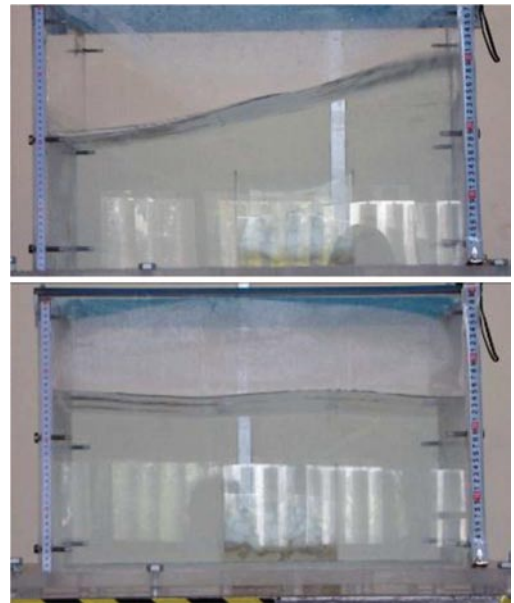


Figure 4. Examples of obtained wave forms: (upper) 1st anti-symmetric mode corresponding to the 1st natural frequency (excitation frequency: 12.9 rad/s, amplitude: 1.9 cm); (lower) 2nd anti-symmetric mode corresponding to the 3rd natural frequency (excitation frequency: 12.13 rad/s, amplitude: 2.1 cm).

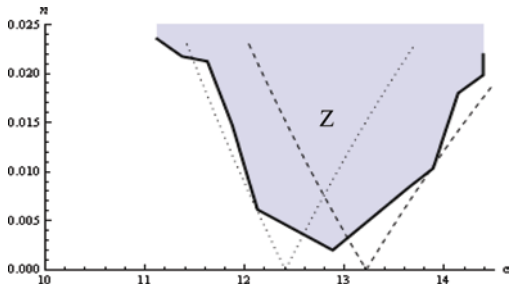


Figure 5. Instability chart (solid line). A comparison is shown against linear theory predictions for the principal parametric instability of the 1st mode (dashed line) and the fundamental instability of the 3rd (dotted line).

In Figure 5 is summarised the region of instability (located to the interior of the solid line), as obtained from the campaign of runs with zero initial conditions. On the graph are superimposed theoretical predictions for the corresponding linear Mathieu-type model of the 1st (dotted line) and 3rd (dashed line) natural mode. The coloured region corresponds to unstable free surface. Theoretical predictions appear well located against the measurements.

Inside the instability area was observed mode competition. It appears that an internal border exists (not shown). To its left, every excitation yields the pattern of the 3rd mode (full wave oscillation); whereas to its right, is realised the 1st mode (half wave oscillation). However, around the border these tests had to be kept on for longer time, until the steady pattern emerged.

#### 4.2 Non-zero initial conditions

In the second series of tests, the same ranges of frequency and amplitude were examined. However, shortly before each run, a short violent roll excitation was applied to the tank, so that the free surface acquires some kind of oscillatory pattern when the parametric excitation was applied. Thus a “non-zero” initial condition was achieved. The obtained picture of the stability region presented notable differences compared to that of the first series. Two were the key findings of this investigation:

- The instability area is much wider compared to that obtained from the first series (Fig. 6). This supplies concrete experimental evidence about the existence of an area where initial conditions affect crucially liquid’s dynamic response.

In Figure 7 is shown a comparison of two qualitatively different steady-state free surface

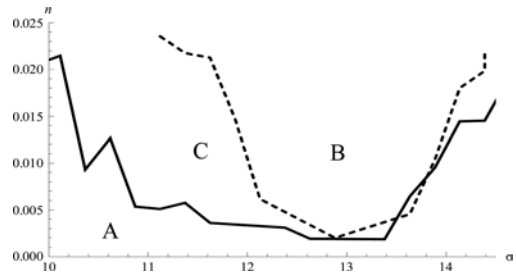


Figure 6. Comparison of experimental results for the two series of tests. Results of the 1st series (zero initial conditions) are indicated by the dashed line while those of the 2nd (non-zero initial conditions) are indicated by the solid line. Area A corresponds to a flat surface steady-state and area B to a wavy one. In area C are hosted the initial-condition-dependent cases.

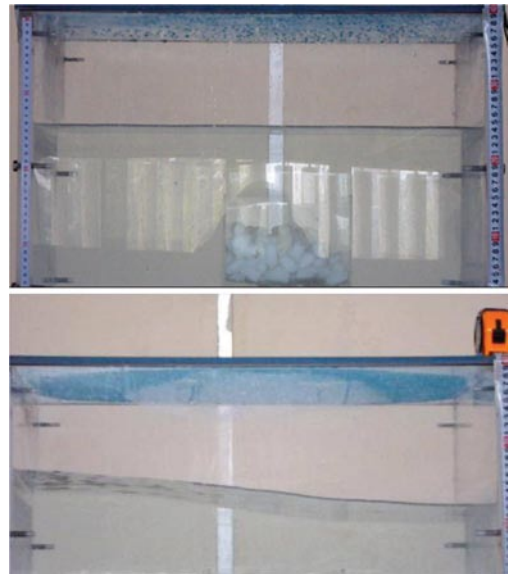


Figure 7. Liquid response obtained for initially horizontal free surface (upper); and for initially disturbed free surface (lower). Excitation frequency and amplitude were 11.7 rad/s and 1.5 cm respectively.

responses obtained inside the bi-stability area (area C). In the upper picture the surface retains the calm water characteristics despite the vertical oscillation of the tank. In the lower picture, the surface oscillates according to the 1st mode.

- A second notable finding is that, inside the bi-stability area C the free surface follows quite different patterns under slightly different excitation frequency and amplitude values.

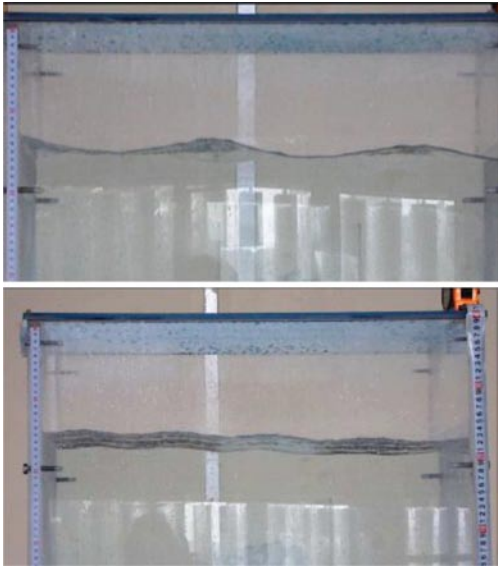


Figure 8. Free surface oscillations in different modes. In the upper picture (obtained with excitation frequency 11.12 rad/s and amplitude 2.1 cm) is captured the 3rd anti-symmetric mode (5th natural frequency). In the lower picture, is captured the 4th anti-symmetric mode (7th natural frequency). The excitation frequency was 14.39 rad/s and the amplitude was 1.7 cm.

In contrast to what happens in area B where purely fundamental and primary resonance of 3rd and 1st mode respectively were observed (as well as evidence of their competition appeared), in area C additional patterns appeared. Specifically, for excitation frequency between 11 and 11.2 rad/s and for amplitude higher than 1 cm the free surface followed sometimes the 5th natural mode (3rd anti-symmetric mode) as shown in Figure 8a. Even higher order natural modes appeared. In Figure 8b is shown a time instance where the 7th natural mode (4th anti-symmetric mode) has appeared. These phenomena possibly have to do with higher resonances of these modes (higher than fundamental). It is noted that double period phenomena are also expected to occur inside the instability area, for high enough excitation amplitudes (Ibrahim 2005).

## 5 EXPERIMENTAL VS NUMERICAL RESULTS

Comparison between the findings from the experiments and from the predictions of our mathematical model is presented in Figure 9. The predictions

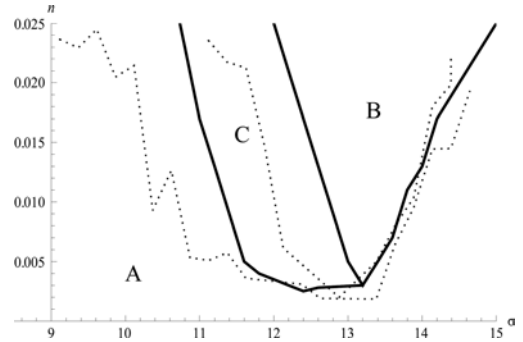


Figure 9. Comparison between numerical (solid line) and experimental (dotted line) results. Instability chart indicating the three different areas.

of the numerical method are in fair agreement with the experimental results. One difference is that the instability area obtained from the experiments is wider. However, the numerical model had been focussed only on the principal resonance of the first mode and furthermore, it was restricted to non-linear terms up to the 3rd order.

Another difference is that the bi-stability area appears wider too in the case of the experiments. This can be understood since higher order natural modes (2nd, 5th and 7th natural modes) were activated in the tests which however were not accounted in the mathematical model. It should be noted that more complex models involving these modes are currently under investigation.

## 6 CONCLUSIONS

By experimental techniques 2-D liquid sloshing in a rectangular, vertically excited tank has been investigated, with focus on validating the prediction of a bi-stability area in parameters' plane. The results obtained from the experiments were compared against numerical results obtained from modal analysis. The investigation was limited to a specific finite liquid depth, corresponding to a tank-height-to-depth ratio of 0.4. The experiments indeed confirm the existence of an area of bi-stability of parametrically excited sloshing. Inside this area, one may obtain a stable wave or a flat surface, depending on the free surface's state when the excitation was firstly applied.

The theoretical predictions are in good qualitative agreement with the real free surface dynamics, despite the assumption of a single dominant mode and the exclusion of the higher order non-linear terms.

A next step towards confirming the capability of the approach to produce more realistic results

will be the investigation of the dynamic behaviour associated with the immediately higher order non-linear model and new validation of these numerical predictions by further series of experiments.

## REFERENCES

- Benjamin T.B. & Ursell F., 1954. "The stability of the plane free surface of a liquid in a vertical periodic motion", *Proceedings of the Royal Society A* 225: 505–515.
- Craik A.D.D. & Armitage J, 1995. "Faraday excitation, hysteresis and wave instability in a narrow rectangular wave tank". *Fluid Dynamics Research* 15: 129–143.
- Decent S.P., 1995. "Hysteresis and mode competition in Faraday waves". Ph.D. thesis, University of St Andrews, Scotland.
- Decent S.P. & Craik A.D.D., 1995. "Hysteresis in Faraday resonance". *Journal of Fluid Mechanics* 293: 237–268.
- Dodge F.T. 1966. Vertical Excitation of Propellant Tanks. In the book: *The Dynamics of Liquids in Moving Containers*. NASA Report SP 106.
- Dhooge A., Govaerts, W., Kuznetsov, Y.A., Mestrom, W., Riet, A.M., Sautois, B., 2003. *MATCONT and CL\_MATCONT: Continuation Toolboxes for MATLAB*, Gent (Belgium) and Utrecht (Netherlands) Universities.
- Faltinsen, O.M. & Timokha, A.N., 2001. "Adaptive multimodal approach to nonlinear sloshing in a rectangular tank", *Journal of Fluid Mechanics*, 432: 167–200.
- Faltinsen, O.M., Timokha, A.N., 2009. *Sloshing*, ISBN: 978-0-521-88111-1, Cambridge University Press, New York.
- Ibrahim, R.A., 2005. *Liquid Sloshing Dynamics*, ISBN: 978-0-521-83885-6, Cambridge University Press, New York.
- International Maritime Organization (IMO), 2012. "Solid Bulk Cargoes Code [IMSBC Code 268(85)]", IMO publishing, ISBN: 978-92-801-1535-2.
- Kityk A.V., Embs JMekhonoshin., V.V., Wagner C., 2005. "Spatiotemporal characterization of interfacial Faraday waves by means of a light absorption technique", *Physical Review E* 72, 036209.
- Miles J.W., 1994. "Faraday waves: rolls versus squares", *Journal of Fluid Mechanics* 269: 353–371.
- Périnet N., Juric D., Tuckerman L.S., 2009. "Numerical simulation of Faraday waves", *Journal of Fluid Mechanics* 635, 1–26.
- Simoneli F & Gollup J.P., 1989. "Surface wave mode interactions: effects of symmetry and degeneracy", *Journal of Fluid Mechanics* 199: 471–494.
- Spandonidis, C & Spyrou K.J., 2011. "Parametric Sloshing in A 2D Rectangular Tank with finite liquid depth". *Proceedings*, 14th International Congress of the International Maritime Association of the Mediterranean (IMAM), Genova, September: 101–108.
- Spandonidis, C.C. & Spyrou K.J., 2012. "Bi-stability in a vertically excited rectangular tank with finite liquid depth", *Ocean Systems Engineering* 2(3): 229–238.